REDUCTION OF BEAM BREAKUP GROWTH BY CAVITY CROSS-COUPLINGS IN RECIRCULATING ACCELERATORS

DENIS COLOMBANT and Y. Y. LAU

Beam Physics Branch, Plasma Physics Division, Naval Research Laboratory, Washington, DC 20375-5000, USA.

DAVID CHERNIN

Science Applications International Corporation, McLean, VA 22102 USA.

It is shown that cross-coupling among cavities may reduce beam breakup (BBU) growth in a recirculating accelerator. The main reason for this growth reduction appears to be the sharing of the deflecting mode energy among coupled cavities. The result is based on a numerical study of the proof-of-principle experiment currently planned for the Spiral Line Induction Accelerator. We conclude that the beam in such an experiment (35 ns, 10 kA, 8.5 MeV) should not be vulnerable to BBU growth. The scalability to much higher energies remains unclear, however, and the various issues are explored.

1 INTRODUCTION

The spiral line induction accelerator (SLIA)[1,2] is a novel compact accelerator with the potential of accelerating a multi-kiloamp electron beam to tens of MeV or beyond. It makes use of a stellarator magnetic field[3] to force the beam to recirculate through the same accelerating unit, and is projected to share many of the advantages of linacs and cyclic accelerators. A proof-of-concept experiment (POCE) is currently under construction.[2] It is designed to trap a 35 ns, 10 kA beam and accelerate it to 8.5 MeV through two recirculations. A schematic drawing of the POCE is shown in Figure 1. It consists of two accelerating units. The beam path threading through these units consists of four arms, labeled sequentially as A, B, C, D. Each of the four arms consists of five accelerating gaps; there are twenty gaps altogether. The gaps in Arm A may electromagnetically be coupled to the gaps in Arm C, and those in Arm B to those in Arm D.

Since beam acceleration occurs only when the beam encounters accelerating gaps, attainment of high energies necessarily requires sequential beam passage through these gaps. Beam breakup (BBU) growth[4–18] is then a primary factor in the ability of the SLIA configuration to achieve ultra-high energies. In addition, it is necessary to devise a new procedure to assess the BBU growth in the POCE, since scalings for such a configuration are unavailable.

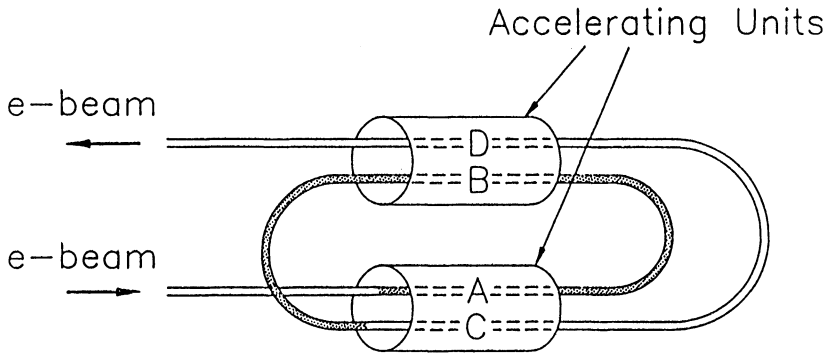# SLIA PROOF–OF–CONCEPT EXPERIMENT

FIGURE 1   Schematic drawing of the Spiral Line Induction Accelerator.

The SLIA is a hybrid between a linac and a cyclic accelerator. BBU growth would occur in the linear sections of the accelerating units where the gaps lie. However, since the beam recirculates through the same accelerating units, albeit via different beam paths (Figure 1), there would be inevitable cross-coupling of the gaps. Thus, the first gap of Arm A would couple to the first gap of Arm C, the second gap of Arm A would couple to the second gap of Arm C, etc. (Figure 2). In fact, there has been considerable concern that such cross-couplings would worsen BBU growth. This concern has prompted consideration of cavity designs that would minimize such cross-couplings.[19] (We will assume here that the beam pipe is cut off to the propagation of the cavity modes responsible for BBU, so that the couplings illustrated in Figure 2 are the only ones possible.)

Since the SLIA is markedly different from a linac, an attempt was made to assess its BBU growth by taking the opposite view, pretending the SLIA to be a strictly cyclic system.[17] That analysis, though not directly applicable to SLIA, does pinpoint some intrinsic differences between BBU in a linac and in a cyclic accelerator.[17,18] It also raised several interesting issues concerning whether BBU growth in a cyclic system is best described in terms of transient amplifications or in terms of unstable eigenmodes, as the properties of growth depend very much on the pulse length, on the number of pulses, on the pulse separation, on the quality factor Q, and on the degree of feedback. Many of these issues remain unsettled.[20]

In this paper, we treat BBU in a SLIA under more-realistic assumptions and employ parameters that cover the range of the POCE. The crucial feature of this work, which is different from all others, is the explicit modeling of cross-coupling of cavities in the different arms of SLIA (Figures 1 and 2). Cavities within the same arm are shielded from one another electromagnetically, as in the POCE. Thus, we may unwrap the SLIA into a linac to treat BBU (Figure 2), except that cavity number 1 is coupled to (and only to) cavity 11, cavity number 2 to number 12, etc. (The twenty cavities are numbered sequentially in the order of beam encounter).

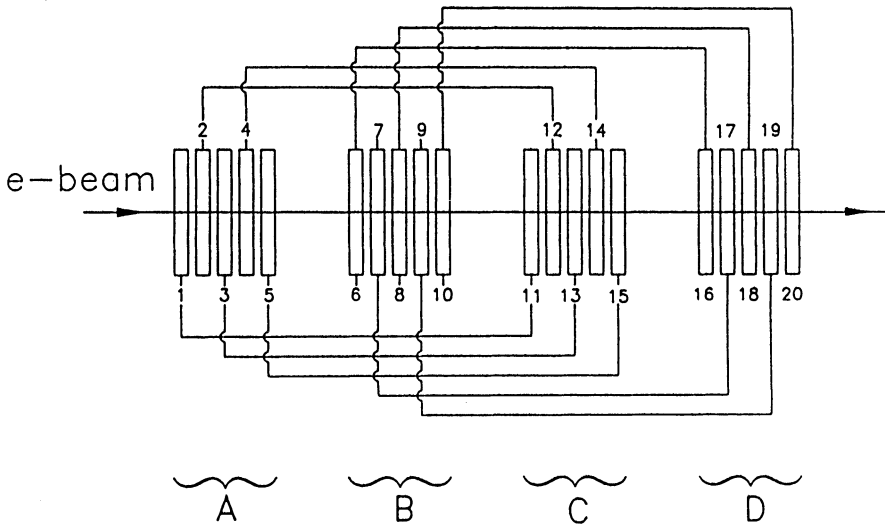# CROSS-COUPLING OF CAVITIES

FIGURE 2 Schematic representation of cross-coupling in the twenty cavities.

The most unusual result that we found is that the presence of cross-coupling may actually reduce BBU growth. Several reasons may be given to explain this unexpected phenomenon: the relatively short pulse length treated, the sharing of the mode energy by another cavity (and therefore the reduction of beam deflection by an individual cavity), and the phase mixing associated with the detuning in the breakup mode frequencies as a result of finite (though small) coupling. This reduction of growth is observed regardless of the value of Q associated with the deflecting dipole mode. Based on this study, we conclude that BBU in the POCE of SLIA is not likely to cause beam disruption.

The following assumptions have been made to reach the above conclusions. All gaps are identical in the sense that, when isolated, each admits a deflecting mode with the same transverse shunt impedance $Z_\perp$ and the same quality factor Q. We assume that cross-coupling would not alter these values. The beam transport between two successive gaps (including that around the bend) is modeled by 2 × 2 matrices[6,7] with constant matrix elements. We consider only a continuous coasting beam, and assume that the beam's pulse length is less than 1/2 of the total transit time from the first cavity to the last cavity so that, at any moment, the beam passes only one cavity in the cross-coupling interaction (Figures 1, 2). We model an individual cavity by an RLC circuit whose natural frequency and Q coincide with the respective values of the deflecting mode. The cross-coupling between the cavities is modeled by a mutual inductance linking the equivalent RLC circuits. This modeling is done in much the same way that cavity coupling is handled in standard microwave litera-ture.[21] The formulation is therefore consistent with the established results in the

appropriate limits: the BBU growth reduces to that of the cumulative BBU in a linac[5,6] when the cross-coupling is absent and the standard coupled cavity result is recovered when the beam is absent.

In Section 2, we describe the cross-coupling of the deflecting modes via simple RLC circuits. There, we introduce the dimensionless cross-coupling coefficient κ. In Section 3, we formulate the governing equations for BBU evolution, including the effects of cross-coupling, together with the imposed boundary conditions and initial conditions. In Section 4, we present the numerical results over a wide range of κ and Q. It is these numerical results on which we base our conclusions, stated in the Abstract. In Section 5, we discuss further the nature of cross-coupling, and examine the possible consequences and implications of relaxing some of the simplifying assumptions. We also raise a number of issues that need to be resolved if the SLIA is to be scaled to much higher energies than the POCE.

2   CROSS-COUPLING BETWEEN CAVITIES

When the gaps are isolated from one another, we assume that the deflecting mode may be modeled by an equivalent RLC circuit of frequency ω_0 and quality factor Q. When cross-coupling between two gaps (cavities) is present, these individual RLC circuits are also coupled. The coupling of cavities has been customarily modeled[21] with a mutual inductance $M \equiv \kappa L$ which links the RLC circuits representing the individual cavities (Figure 3). Here, κ is the dimensionless constant which measures the degree of (cross-) coupling. When the coupling is weak,
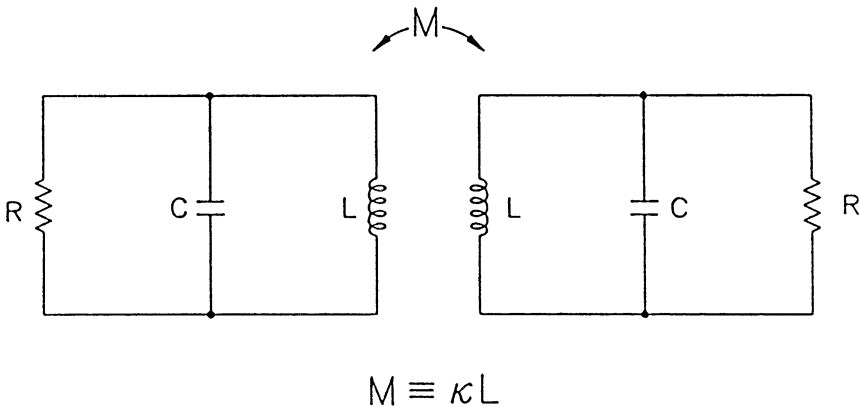
$$\kappa \ll 1. \tag{1}$$

MODEL OF CAVITY COUPLING

FIGURE 3   Circuit model for cavity cross-coupling.

We assume that the presence of cross-coupling does not alter the values of Q and $Z_\perp$ of the deflecting mode in an isolated gap. Thus, $\omega_0 = 1/\sqrt{LC}$ and $Q = \omega_0 RC$.

To account for the cross-coupling between, say, cavity 1 of arm A and cavity 11 of arm C (Figure 2), we first denote $f^{(i)}(t)$ to be the deflecting mode amplitude of the i-th cavity at time t. When the weak coupling condition (1) is satisfied, $f^{(1)}$ and $f^{(11)}$ may be shown to be governed by the following differential equations when the beam is absent (see Appendix A):

$$Lf^{(1)}(t) = \kappa\omega_0^2 f^{(11)}(t) \tag{2}$$

$$Lf^{(11)}(t) = \kappa\omega_0^2 f^{(1)}(t), \tag{3}$$

where L denotes the operator

$$L \equiv d^2/dt^2 + (\omega_0/Q)d/dt + \omega_0^2. \tag{4}$$

Equations (2) and (3) admit normal solutions of the form $\exp(i\omega t)$. When $\kappa = 0$ (zero coupling), both $f^{(1)}(t)$ and $f^{(11)}(t)$ oscillate independently with

$$\exp(i\omega_0 t - \omega_0 t/2Q)$$

dependence. When $\kappa^2 \ll 1$, the eigenfrequencies are given by

$$\omega = \left[\frac{i}{2Q} + \left(1 \pm \frac{\kappa}{2}\right)\right]\omega_0. \tag{5}$$

Equation (5) shows that the coupling leads to a slight detuning of the breakup mode frequency and that there are two independent modes of oscillation.[22]

The coupling between cavity number 2 and number 12 is also descibed by Eqs (2) and (3), in which $f^{(1)}$ is replaced by $f^{(2)}$ and $f^{(11)}$ by $f^{(12)}$. A similar procedure applies to coupling between cavity number 3 and cavity number 13, and so on.

We have assumed that there is no phase shift in the coupling between cavity number 1 and cavity number 11. If the two cavities are symmetrically placed within the cross section of the acceleration unit, the phase shift should, by a symmetry argument, be either zero or π. The case of phase shift equal to π is equivalent to replacing κ in Eqs (2) and (3) by $-\kappa$. Even in the presence of the beam, we have found from the numerical results that the BBU growth is not sensitive to the sign of κ. Henceforth, we take $\kappa \geq 0$.

It is of interest to note at this point that the presence of cross-coupling leads to two distinct modes, associated with the $\pm$ sign in Eq. (5). Thus, the beam needs to drive *two* modes (instead of *one* when such a coupling is absent). For the same beam deflection, the deflecting mode amplitude in a cavity would be less when $\kappa \neq 0$. This reduction in deflecting mode amplitude would in turn produce less transverse displacement of the beam. We believe that the above processes constitute the main reason why cross-coupling reduces BBU growth, at least within the context of the present model of cavity coupling.

Finally, we remark that the "leakage" of mode energy to another cavity (when $\kappa \neq 0$) is not equivalent to an effective lowering of Q in the present model of cross-coupling. A finite Q always represents lossy processes from which energy cannot

be recovered, whereas a nonzero κ represents only reactive loading which does not result in any energy loss. This is obvious in the coupled circuit shown in Figure 3. To see this mathematically, we set $Q = \infty$ (i.e., remove the lossy processes) but keep $\kappa \neq 0$ in Eqs (2), (3). These two equations imply conservation of total mode energy because of the self-adjointness of the operator L when $Q = \infty$. The remaining question, which we shall not address in this paper, concerns the condition under which cavity cross-coupling can be modeled by the coupled-mode treatment given in this section. The alternative would be to treat the entire accelerating unit, including all of the gaps on the various arms threading through the unit, as a single resonant structure.

3   FORMULATION OF BEAM BREAKUP GROWTH IN THE PRESENCE OF CAVITY CROSS-COUPLING

This formulation of beam-gap interaction follows closely those given in the BBU literature. Consider a uniform coasting beam of pulse length τ, relativistic mass factor γ, and current I. Let $x^{(i)}(t)$ and $p^{(i)}(t)$, be respectively, the transverse displacement and the transverse momentum of a beam slice that, at time t, is about to enter the ith accelerating gap ($i = 1, 2, \ldots, 20$). Let $x_+^{(i)}(t)$ and $p_+^{(i)}(t)$ be the corresponding quantities when this beam slice exists the ith gap. If the gap width is small, then[5,6]

$$x_+^{(i)}(t) = x^{(i)}(t) \tag{6}$$

$$p_+^{(i)}(t) = p^{(i)}(t) + f^{(i)}(t), \tag{7}$$

where $f^{(i)}(t)$ is the incremental momentum produced by the deflecting mode at the ith cavity at time t. The ith cavity is in turn excited by the beam's transverse displacement, and, because of the cross-coupling, it is also excited by the neighboring cavity which lies on the same plane orthogonal to the beam path. Referring to Eqs (2) and (3), the evolution of $f^{(i)}(t)$ is governed by[6,17]

$$Lf^{(i)}(t) = \frac{e}{c^3} \omega_0^3 I\left(\frac{kc}{\omega_0}\right) h^{(i)}(t) x^{(i)}(t) + \kappa \omega_0^2 f^{(j)}(t); \tag{8}$$

$$i = 1, 2, \ldots, 20$$

where $j = i + 10$ if $i \leq 10$ and $j = i - 10$ if $i \geq 11$.

In Eq. (8), (kc/ω_0) is a dimensionless quantity equal to $Z_\perp(\Omega)/30\,Q$ [Ref. 6], and

$$h^{(i)}(t) = \begin{cases} 1, & t_i < t < t_i + \tau \\ 0, & \text{otherwise} \end{cases} \tag{9}$$

represents the time interval during which the beam passes through the ith gap. We have used t_i to designate the time at which the beam head enters the ith gap. If T designates the transit time between neighboring cavities within the same arm and T' the transit time to go around each bend (e.g., from cavity no. 5 to cavity no. 6), then $t_1 = 0, t_2 = T, t_3 = 2T, t_5 = 4T, t_6 = 4T + T', t_{12} = 9T + 2T'$, etc. (Figure 2).

We next assume that the beam transport between neighboring cavities within the same arm can be modeled by a 2×2 matrix A.[6] In general, a different matrix A' would be necessary to model beam transport across the bend.[7] Thus, the beam transport within the same arm is described by

$$\begin{bmatrix} x^{(i+1)}(t+T) \\ p^{(i+1)}(t+T) \end{bmatrix} = A \begin{bmatrix} x_+^{(i)}(t) \\ p_+^{(i)}(t) \end{bmatrix} = A \begin{bmatrix} x^{(i)}(t) \\ p^{(i)}(t) + f^{(i)}(t) \end{bmatrix} \tag{10}$$

for $i \neq 5, 10, 15$. Across the bends,

$$\begin{bmatrix} x^{(i+1)}(t+T') \\ p^{(i+1)}(t+T') \end{bmatrix} = A' \begin{bmatrix} x_+^{(i)}(t) \\ p_+^{(i)}(t) \end{bmatrix} = A' \begin{bmatrix} x^{(i)}(t) \\ p^{(i)}(t) + f^{(i)}(t) \end{bmatrix} \tag{11}$$

for $i = 5, 10, 15$. In writing the last forms of Eqs (10) and (11), we have used Eqs (6) and (7).

Equations (8), (10) and (11) are the governing equations for the transverse displacement $x^{(i)}(t)$, transverse momentum $p^{(i)}(t)$, and the deflecting mode amplitude $f^{(i)}(t)$. The following initial conditions and boundary conditions are imposed. We assume that the beam enters the first cavity without any initial transverse displacement nor transverse momentum. For the cavities, we assume that, at $t = 0$, they are all unexcited, except the first one, which has an amplitude f_0 at $t = 0$. Thus, the only non-trivial initial condition is

$$f^{(1)}(0) = f_0 = \text{non-zero constant.} \tag{12}$$

All remaining initial conditions are set to zero.

4 NUMERICAL RESULTS

In the presentation of the numerical results, we shall use the normalized time variables $\bar{t} = \omega_0 t$. We shall normalize both p and f with respect to f_0, the initial amplitude of the deflecting mode in the first cavity, cf. Eqs (12) and (7). The diagonal elements of the transport matrices A and A' are always dimensionless. The off-diagonal ones become dimensionless if we normalize p by f_0. We shall use the normalized variables, unless otherwise specified. The normalized equations are given in Appendix B.

In these normalized variables, the breakup mode period in the individual cavity is 2π. We set $\omega_0 T = 7.33$, $\omega_0 T' = 73.3$, and $\omega_0 \tau = 204$ in all numerical calculations. Note that the pulse length is sufficiently short that, at any instant, only one (not both) of the cross-coupled cavities is occupied by the beam. The above numbers correspond to a breakup mode frequency of 1 GHz, a cavity separation within each arm of 35 cm, and a distance around bend (from Gap 5 to Gap 6) of 350 cm. To characterize the BBU interaction with a gap, we introduce a dimensionless parameter

$$\varepsilon_r \equiv \frac{1}{\gamma} \left(\frac{I}{17 \, \text{kA}} \right) \left(\frac{kc}{\omega_0} \right), \tag{13}$$

which measures the strength of BBU excitation within each gap (cf. Eq. (B3) of Appendix B). For $I = 10$ kA, $\gamma = 17$, $kc/\omega_0 = 0.416$, we have $\varepsilon_r = 0.0144$. This value of ε_r has been used in all numerical calculations.

Finally, for the transport matrices, we assume that, for simplicity, the effective betatron frequencies ω_c associated with beam transport within the straight arms A, B, C, D are identical to those in the bends. We shall use $\Omega \equiv \omega_c/\omega_0$ to denote focal strength. Note that if $\omega_0/2\pi = 1$ GHz, Ω would assume a value of 0.28 if the effective betatron wavelength $2\pi c/\omega_c$ is 1.07 meter. For $\Omega = 0.8$, the elements $\bar{a}_{ij}$ in the normalized matrix $\bar{A}$ are $\bar{a}_{11} = \bar{a}_{22} = 0.9134$, $\bar{a}_{12} = -0.509$, $\bar{a}_{21} = 0.326$, whereas those in $\bar{A}'$ are: $a'_{11} = \bar{a}'_{22} = -0.462$, $\bar{a}'_{12} = 1.11$, $\bar{a}'_{21} = -0.462$. (See Appendix B).
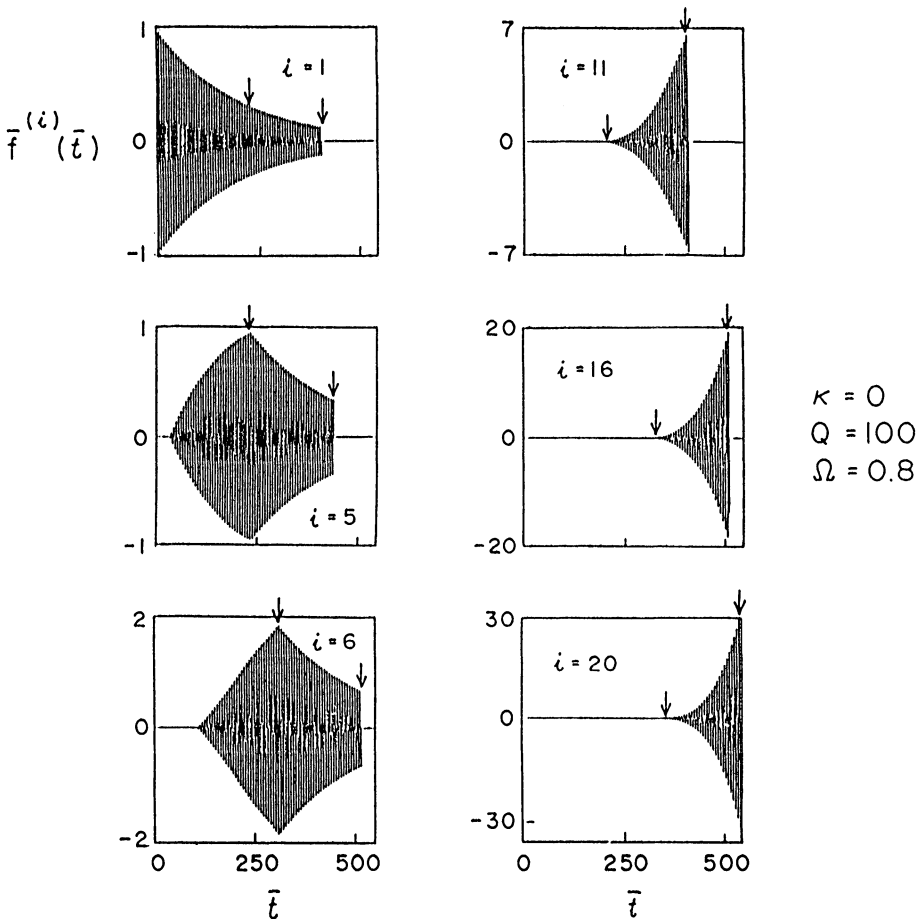

FIGURE 4 Evolution of the deflecting modes $\bar{f}^{(i)}(\bar{t})$ at the ith cavity. In the left column ($i = 1, 5, 6$), the arrows on the left designate the time at which the entire beam exits the ith cavity; the arrows on the right designate the time when the whole beam exits the $(i + 10)th$ cavity. In the right column ($i = 11, 16, 20$), the arrows on the left designate the time of arrival of the beam head at the ith cavity; the arrows on the right designate the time when the entire beam clears the ith cavity. The values of Q, κ, and Ω are specified on the figure. The coordinates have linear scales.

In the numerical calculations, the parameters we have used are $Q = 4, 20, 100, 10^4$; $\Omega = 0.14, 0.28, 0.8$; and $\kappa = 0, 0.01, 0.03, 0.1, 0.3$. These numbers span a rather wide range. (The data for $\kappa = 0.3$ are included only to show the qualitative behavior when substantial cavity cross-coupling is present. One may argue that the mode coupling formulation is adequate only for $\kappa \leq 0.1$).

In order to read the figures in more detail, we make a few comments about the dimensionless time coordinate in Figures 4–9. In these units, the beam enters cavity 1 at $\bar{t} = 0$ and cavity 11 (the cavity to which it is connected) at $\bar{t} = 206$. It enters cavity 5 at $\bar{t} = 30$, cavity 6 at $\bar{t} = 103$ (after a bend), cavity 16 at $\bar{t} = 310$ (cavity 16 is cross-coupled to cavity 6) and cavity 20 at $\bar{t} = 340$. The beam's pulse length is 204 time units.
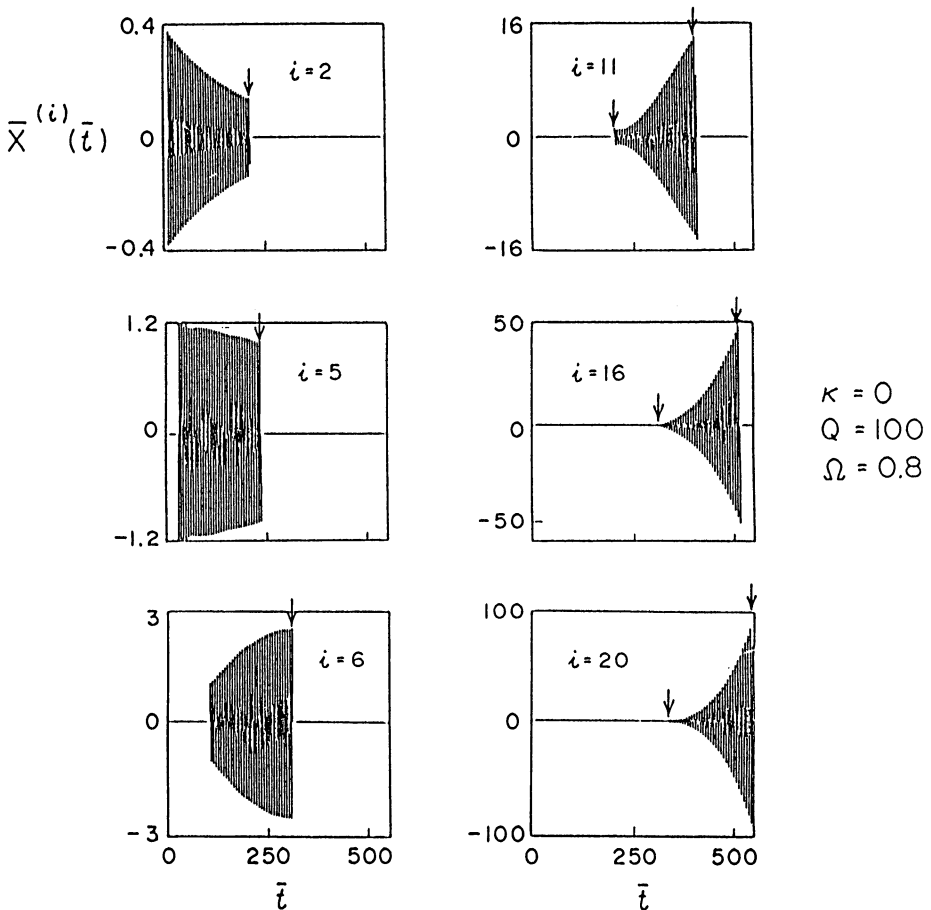

FIGURE 5   The evolution of the normalized transverse displacement $\bar{x}^{(i)}(\bar{t})$ at the ith cavity. The arrows in the left column ($i = 2, 5, 6$) designate the time at which the entire beam leaves the ith cavity. In the right column ($i = 11, 16, 20$), the arrows on the left designate the time of arrival of the beam head at the i-th cavity; the arrows on the right designate the time at which the entire beam leaves the ith cavity.
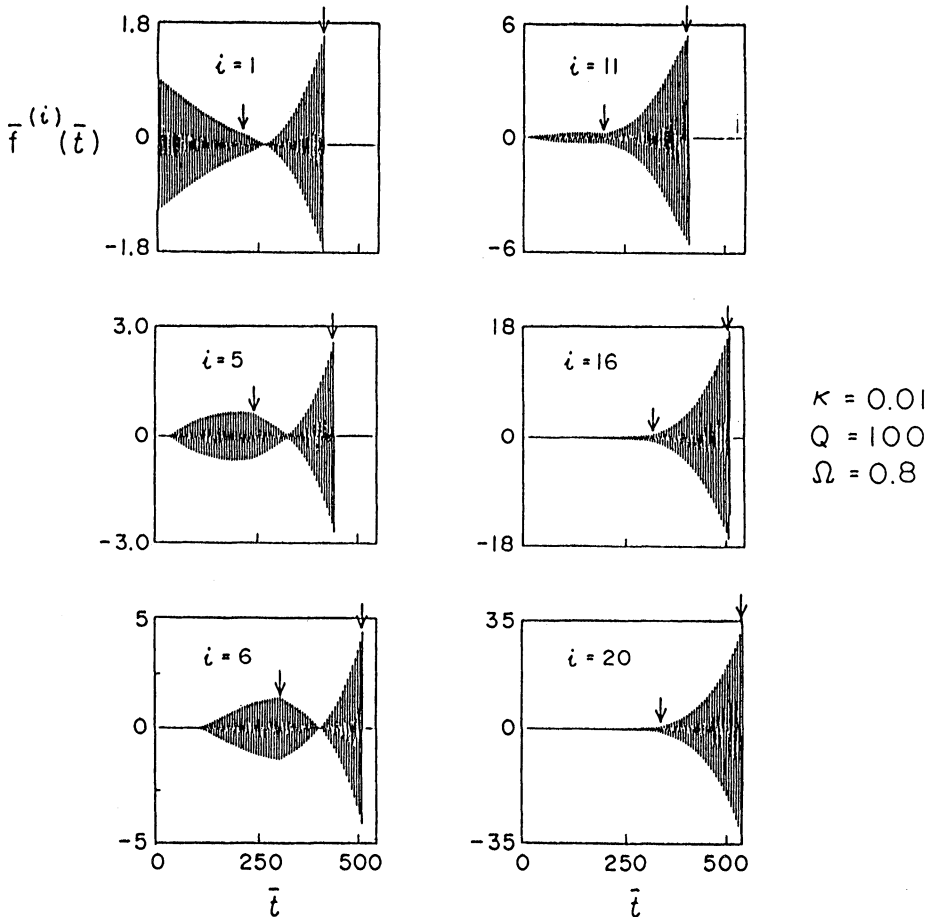
FIGURE 6   Same as in Figure 4.

In Figures 4 and 5, data for the case $Q = 100$, $\kappa = 0$ (no cross-coupling), and $\Omega = 0.8$ are presented. Figure 4 shows the deflecting mode amplitude in cavities 1, 5, 6, 11, 16 and 20. Figure 5 shows the beam transverse displacement in the same cavities. We see in Figure 4 that the deflecting mode decays continuously with time in cavity 1 as expected because of the finite Q; cavity 1 is not excited by the beam since the beam enters on axis, by assumption. This decay continues until the beam has left the (un)coupled cavity 11, beyond which time it presents no physical interest to either cavity 1 or 11. The field in cavity 5 shows a different pattern. No field is present in the cavity before beam entry and the field rises in the cavity due to its excitation by the beam. As soon as the beam leaves the cavity, the field decays as in cavity 1. This pattern is actually repeated in cavities 2 through 10. The pattern in cavities 11 through 20 is not physically different but appears differently in the figure. In these graphs, only the rise in field amplitude is shown, since the decay is not relevant, the beam not re-entering any cavity coupled to those. Note that in this case
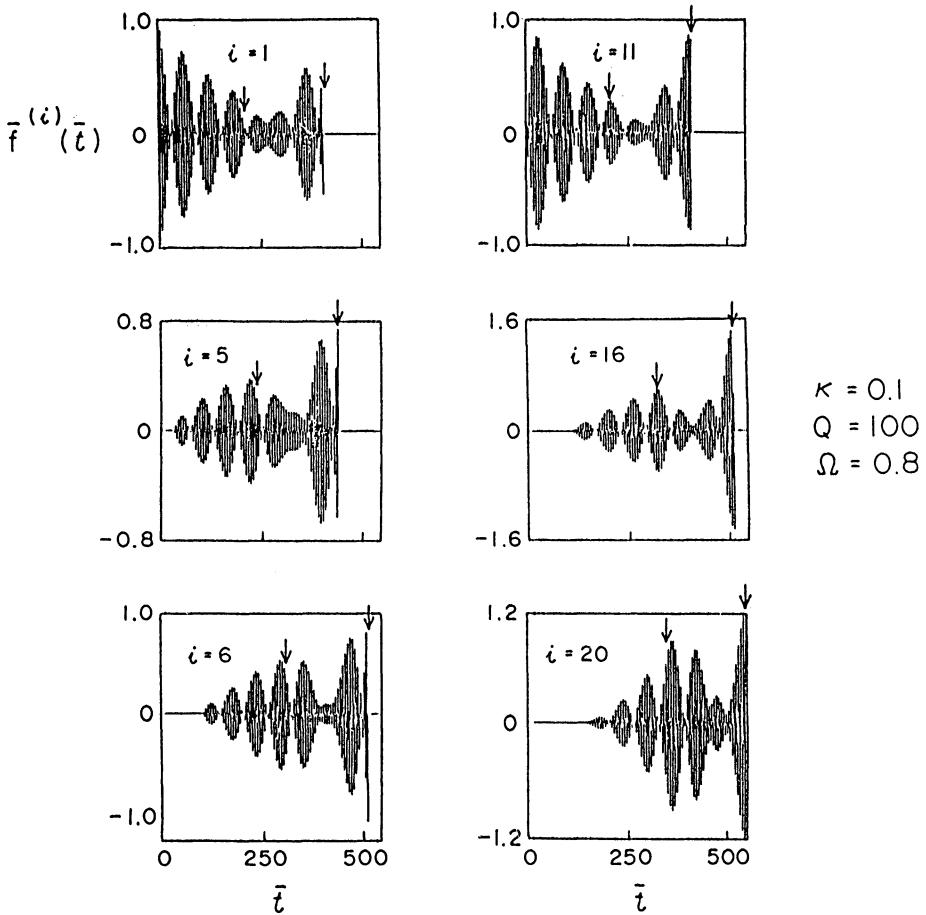
FIGURE 7   Same as in Figure 4.

of no cross-coupling, the field amplitude is always zero before the beam enters the cavity, except in cavity 1, by assumption.

The beam transverse displacement does not show as much structure since the beam goes only once through each cavity. Figure 5 shows the displacement in the same cavities as in Figure 4, except for cavity 1, which has been replaced by cavity 2 (the displacement in cavity 1 is always zero). The beam picks up a non-trivial transverse displacement only when it arrives at cavity 2. This "initial" displacement is equal to $x_0 = \bar{a}_{12} = \Omega^{-1} \sin(\Omega\bar{T})$, cf. Eq. (B-11) of Appendix B. In order to assess BBU growth, we take the ratio of the final beam displacement to this initial displacement (Figures 10, 11). The beam displacement in Figure 5 does not evolve exactly as the field amplitude in Figure 4 but it can be seen to decay in the first cavities before growing exponentially as expected of BBU. For the present case, the transverse displacement reaches 228 times its initial displacement after 20 cavities.
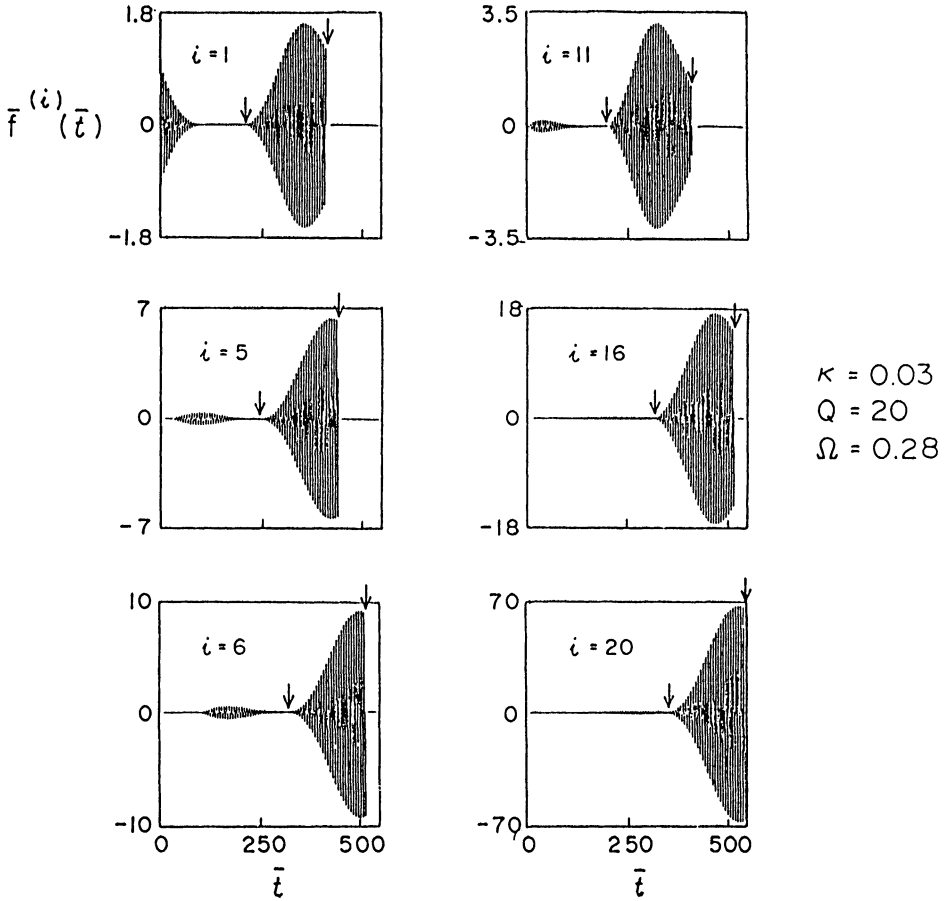
FIGURE 8   Same as in Figure 4.

The cavity modes shown in Figure 6 correspond to the same Q, ε_r and Ω as in Figure 4 but include a small cross-coupling $\kappa = 0.01$. Although the final transverse displacement is similar (228 x_0 vs. 210 x_0), the mode evolution is qualitatively very different. The difference starts with cavity 1, for example, where the field decays at first. However, once the beam enters the coupled cavity 11, leakage from that cavity, although not very important, shows very clearly in the rise of the field in cavity 1. Although this field will not act on any part of the beam directly in the present configuration, it is important to evaluate it since it affects the field in cavity 11, which is itself driving the beam. The pattern shows very clearly for cavities 5 and 6. In cavity 11, another difference appears. In that cavity, when the beam enters it at $\bar{t} = 206$, the field is non-zero since it was leaked from cavity 1 from $t = 0$ onward. It was thought that this non-zero field could aggravate BBU growth but it turns out that the opposite conclusion is reached — namely, that this non-zero leakage actually alleviates BBU. This apparently contradictory result will be addressed further in the next section.
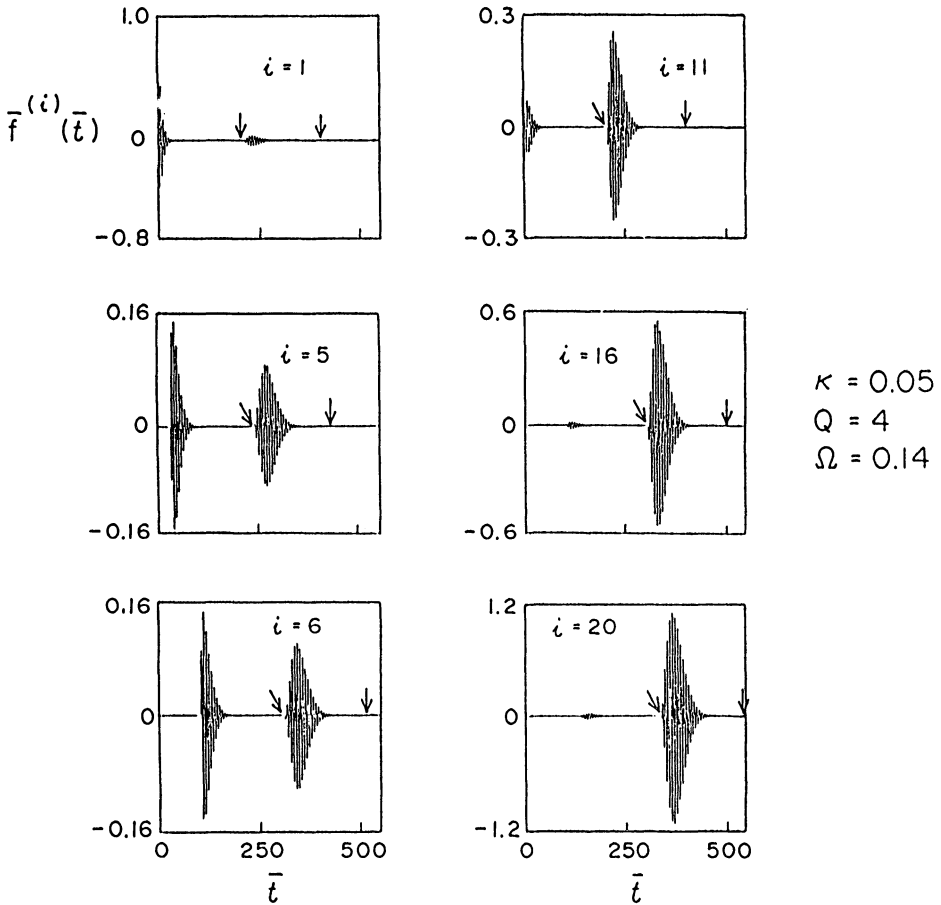
FIGURE 9 Same as in Figure 4.

Differences in beam behavior are much smaller than differences in field amplitudes, and, in fact, beam displacement is quite similar to the $\kappa = 0$ case and will not be shown. As the cross-coupling constant increases, the coupling between modes in corresponding cavities increases and, as shown by Eq. (5), two modes would be excited and their beatings give rise to much more complex time behavior. This type of behavior is evident in Figure 7, as an example, where $\kappa = 0.1$. It is apparent, by comparing Figure 4 and Figure 7, that increasing the coupling coefficient κ reduces BBU growth.

Runs have been repeated for the case $Q = 20$, $\Omega = 0.28$ (Figure 8) and for $Q = 4$ and $\Omega = 0.14$ (Figure 9). The decreasing values of Ω correspond to decreasing values of the focal strength. These two cases display behavior similar to the higher Q case shown in detail previously. The maximum beam transverse displacement at cavity 20 normalized to its initial displacement is shown as a function of κ for these cases in Figures 10 and 11. The effect of cross-coupling is evident. However, it becomes less important as Q decreases. This can be explained easily, since for low Q, the modes
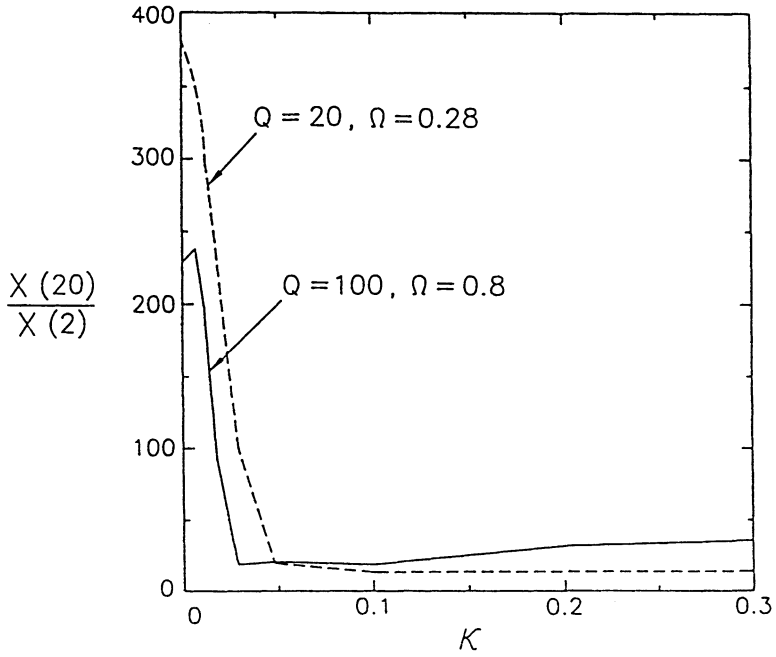
FIGURE 10   The ratio of the maximum transverse displacements at cavity no. 20 and at cavity no. 2, as a function of κ, for the values of Q, Ω specified in the figure.
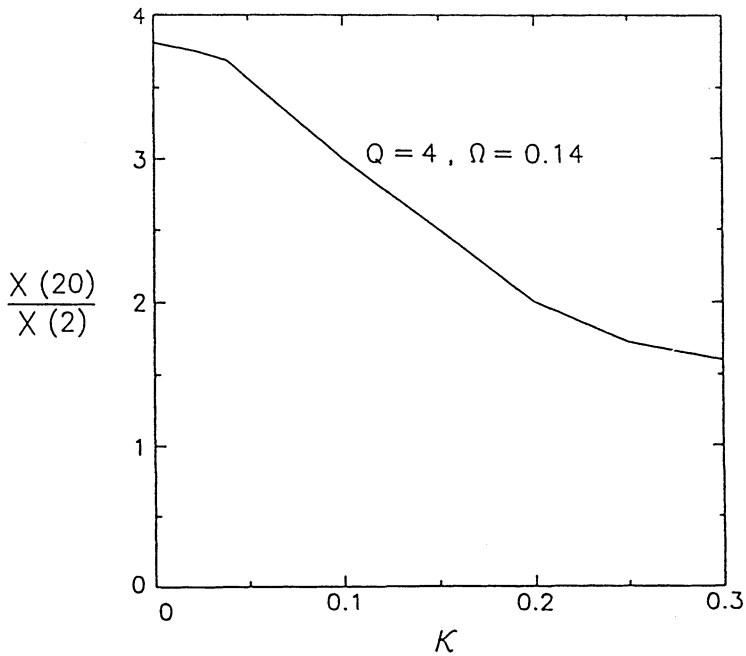

FIGURE 11   Same as in Figure 10.

are damped much more effectively and by the time the beam enters a coupled cavity the fields in that cavity will decay to a low level. (see Figure 9). Basically, a low-Q cavity is not very different from an uncoupled one, and this fact is borne out by the results. Figure 12 shows the peak mode amplitudes as a function of κ, in several cavities for the case $Q = 100$.

We have considered three different values of Q because, although the dominant break-up mode may have a low-Q value, the residual deflecting modes may have much higher Q values and it is those modes that are most difficult to control. However, although the reduction in growth is larger for higher-Q cavities, final beam displacement is still larger for these modes. There is substantial reduction in the transverse displacement by factors of ten or more, when the coupling constant κ exceeds a few percent.

One may question whether the BBU growth reduction by cavity cross-coupling is merely a coincidence due to the specific values assigned to the breakup mode frequency and to the focal strength. To answer this question, we have varied the breakup mode frequency ω_0, fixing all other parameters, such as ω_c, T, T', τ, I, and γ. Specifically, we have changed ω_0 by about 5 percent, so that $\omega_0\tau'$ ranges from $(206 - 2\pi)$ to $(206 + 2\pi)$, where τ' is the transit time of a beam slice to travel
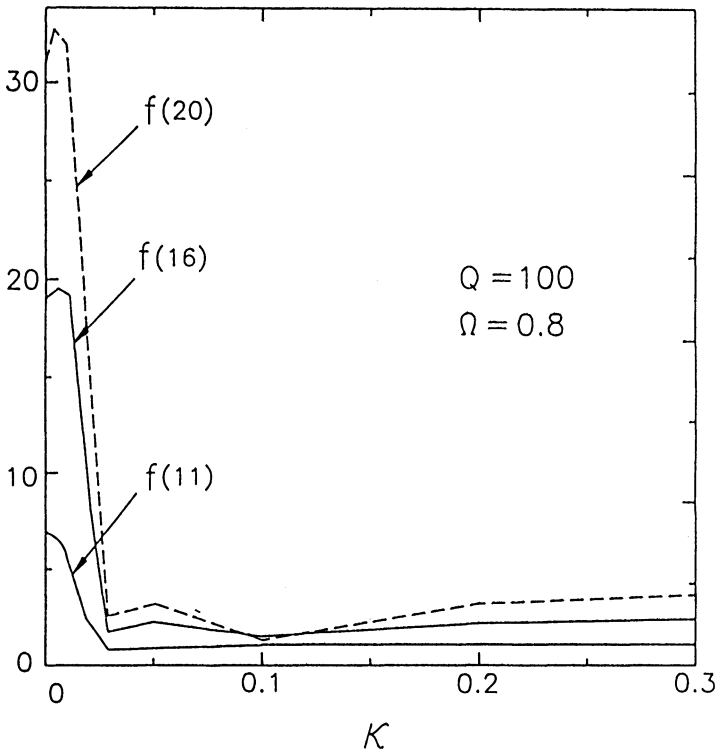

FIGURE 12   The maximum mode amplitude at cavities nos. 11, 16, 20 as a function of κ. Here $Q = 100$, $\Omega = 0.8$.

between each pair of cross-coupled cavities, e.g., between cavity 1 and cavity 11. Thus, the phases of electron arrival at the cross-coupled cavity may take on any value over two breakup mode cycles. (We chose two breakup cycles to make sure that the result is essentially unchanged from one cycle to another, as shown by the solid curve in Figure 13). The comparison between the $\kappa = 0.03$ and the $\kappa = 0$ case is shown in Figure 13. This figure gives the maximum beam deflection $\bar{x}(20)$ at the last cavity as a function of $\omega_0 \tau'$ over the interval $(206 - 2\pi) < \omega_0 \tau' < (206 + 2\pi)$. We have set $Q = 100$ and, when $\omega_0 \tau' = 206$, $\Omega = 0.8$. We see that $\bar{x}(20)$ without cross-coupling (the $\kappa = 0$ case) is always higher than that for the $\kappa = 0.03$ case, by at least a factor of 6. Thus, growth reduction by cavity cross-coupling is prevalent and the phase variation in $\omega_0 \tau'$ does not seem to negate such features. We believe that this relative insensitivity to the phase is a result of the relatively short pulse length treated. (Figure 13 shows that the phase variation can produce a 50 percent variation in $\bar{x}(20)$ for the $\kappa = 0.03$ case).
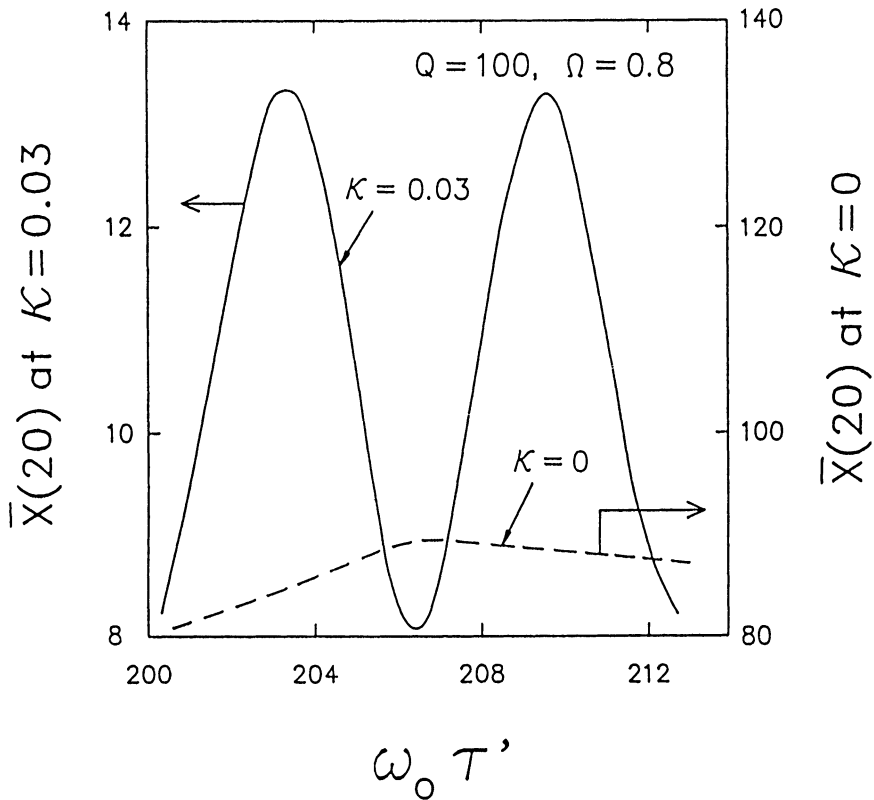

FIGURE 13   The maximum normalized transverse displacement $\bar{x}(20)$ as a function of $\omega_0 \tau'$, which is the phase advance in the breakup mode during the time interval it takes a beam slice to travel between cross-coupled cavities. Note that growth reduction persists for the $\kappa = 0.03$ case (when compared with the $\kappa = 0$ case), regardless of this phase.

We summarize the main features in the above analysis.

1) BBU growth decreases with increasing cross-coupling between cavities.

2) Significant growth reduction occurs when $\kappa >$ a few percent.

3) The reduction in BBU amplitude can be a factor of 10 or more.

4) Substantial growth reduction is achieved for a large range in κ values and so should be readily implemented experimentally.

5) The growth reduction persists, irrespective of the phase of electron arrival at the cross-coupled cavity.

These features are rather significant because they show a possible reduction in BBU growth in a recirculation system which is not available in a linac geometry.

Based on the above findings, we now compare BBU growth in a cyclic accelerator, in a linac, and in a recirculating linac with cross-coupling. Strictly cyclic systems admit unstable normable mode solutions (for a given cavity) with simple exponential growth in time.[17,18] Cumulative BBU in a linac exponentiates at a fractional power of time[5,6,13–16,23,24] ($\leq 1/2$) and it therefore may be said to be less virulent. Here, we have shown that BBU growth may further be reduced with cross-coupling of cavities in a recirculating geometry, such as SLIA.

5 DISCUSSIONS

The numerical results based on the rudimentary theory led to the following. First, the proof-of-concept experiments in SLIA as currently planned are not likely to be vulnerable to BBU. Second, contrary to customary thinking, cross-coupling of cavities in different arms of the SLIA is found to reduce BBU growth. Since the second point is rather unusual, we shall have to explore further the implications. We shall also comment on the limitations of our model and raise the various issues that need to be addressed if SLIA is to be scaled to much higher energies.

We can name two reasons why cross-coupling among cavities could reduce BBU growth. First, when coupling is present, the energy in one cavity is shared with another cavity. Thus the cavity does not exert as strong a transverse deflection on the beam. In addition, the beam needs to excite both cavities when cross-coupling is present. For the same transverse displacement of the beam, the deflecting mode that would be excited in an individual cavity has a lower amplitude. Based on this simple physical argument, it is natural to speculate that the BBU gain per pass would be further reduced if each accelerating unit were to accommodate a large number of arms. In such a case, the deflecting mode energy in one cavity is shared by a large number of other cavities through mutual cross-coupling. This scenario is quite plausible if the beam's pulse length is short enough so that, at any instant, the beam resides in only one of the various arms in the cross-coupling interaction. Should this be the case, we have here a rather peculiar situation for SLIA: the BBU growth per pass is reduced as the number of recirculations is increased.

The result that mode-coupling can reduce BBU growth may be extended to linacs. If the accelerating cavities in a linac are coupled to similar but undriven cavities, BBU growth may be reduced due to the reactive loading by these dummy cavities. (See the last paragraph in Section 2).

Returning to the present study, we note that even if there is pre-existence of a deflecting mode in a given cavity prior to beam arrival due to cross-coupling, this initial mode energy does not seem to reverse the beneficial effects of cross-coupling, as discussed above. Our numerical calculation has been extended to very high Q values ($Q = 10^4$) and these conclusions remain valid. Equation (5) suggests the existence of two distinct modes when $\kappa \neq 0$. A close examination of the numerical results shows that the solution is biased toward the slow mode $\omega \simeq \omega_0(1 - \kappa/2)$ when BBU is excited.

The second, but perhaps less convincing, reason is that the presence of cavity coupling leads to a detuning of the breakup mode frequency, cf. Eq. (5). This detuning may loosely be associated with an intrinsic frequency spread which is known to provide phase mixing. This in turn leads to reduction of BBU growth.[14,15,23]

We shall now address the deficiencies in our model and speculate on their effects on the BBU growth. We have assumed that the values of Q and $Z_\perp$ associated with a single, isolated cavity remain unchanged when this cavity is coupled to another. The adoption of this assumption may have already led to an overestimate of the BBU growth since, intuitively, when the energy within one cavity is allowed to couple to another, $Z_\perp$ would be reduced, as it is a measure of the excitability of the cavity by a traveling electron that is displaced from the center axis of the cavity. Other simplifying assumptions we have made include a coasting beam and the use of constant 2×2 matrices to model beam transport between cavities (including bends). The dependence of BBU on γ, which varies with the focusing system, is relegated to a secondary role.

Let us now consider the various BBU issues that need to be addressed if the SLIA is extended to an energy much beyond 8.5 MeV (as planned in the POCE). In that case, many more recirculations and/or higher gain per arm would be required, and each beamlet would encounter a large number of cavities. The cross section of an acceleration unit would accommodate many arms of the beam pipe. The cross-couplings among these various arms are clearly far more complex, though they may lead to reduction of BBU gain per pass. This argument actually depends on whether the beam consists of one single pulse or a series of pulses. It is possible that our conclusion regarding BBU reduction by cavity cross-coupling would be altered, for example, in the case of multiple pulses. One can think of situations in which cavity cross-coupling may worsen BBU growth in a recirculating geometry, especially when the individual beam pulses *simultaneously* occupy the various arms within the same acceleration unit. In the latter case, the BBU growth would also show considerable phase sensitivity, in sharp contrast to that displayed in Figure 13. These issues remain to be investigated.

As we have emphasized, SLIA is neither a linac nor a strictly cyclic system. Applicable scaling laws are non-existent at the time of this writing. They would be highly desirable but their derivation touches upon some rather complex mathematical

issues. Chief among them is the question of whether conditions exist under which BBU in SLIA would evolve in a transient manner, or into an unstable normal mode (if there is one).

There are other important topics that have not been addressed. They are mainly related to ultra-high-energy SLIA operation. For example, the numerous encounters of the beam with gaps require closer attention to the coupling between BBU and orbital resonances.[24] Perhaps more importantly the many recirculations of a high current beam may dangerously couple the negative mass[25] and image displacement instabilities to BBU. These couplings cannot be ignored if the SLIA is to be extended to the multi-kiloamp, hundred-MeV range.

ACKNOWLEDGEMENT

APPENDIX A

MODEL EQUATIONS FOR THE COUPLED CAVITIES

Consider first the coupling of the two identical RLC circuits (labeled a, b), as shown in Figure 3. These two circuits are linked by a mutual inductance

$$M \equiv \kappa L \tag{A1}$$

where $\kappa \ll 1$ is the dimensionless coupling constant. Let V_a be the voltage across the inductance L of circuit "a" and I_a be the current flowing through this inductance. Let V_b and I_b be the corresponding quantities for the inductance of circuit "b". Assume solutions with exp $(i\omega t)$ dependence. The definition of mutual inductance M gives

$$V_a = i\omega L I_a + i\omega M I_b \tag{A2}$$

$$V_b = i\omega L I_b + i\omega M I_a \tag{A3}$$

We next apply the Kirchoff current law to circuits "a" to yield

$$I_a + \frac{V_a}{R} + i\omega C V_a = 0. \tag{A4}$$

Similarly, for circuit "b",

$$I_b + \frac{V_b}{R} + i\omega C V_b = 0. \tag{A5}$$

The four Eqs (A2)–(A5) in the four unknowns V_a, V_b, I_a, I_b yield the natural frequencies of oscillation of the coupled circuits:

$$\omega = \omega_0\left[1 + \frac{i}{2Q} \pm \frac{\kappa}{2}\right]. \tag{A6}$$

In writing Eq. (A6), we have ignored quantities of order κ^2 and $1/Q^2$, and we have used the relation $\omega_0^2 = 1/(LC)$ and $Q = \omega_0 RC$. The two modes given in Eq. (A6) have obvious interpretations in the $Q \rightarrow \infty$ limit and in the $\kappa \rightarrow 0$ limit.

The cross-coupling between the cavities shown in Figure 2 may now be described, making use of the preceding results. For example, let circuit "a" represent cavity no. 1 and circuit "b" represent cavity no. 11 of Figure 2. The field amplitudes $f^{(1)}(t)$ and $f^{(11)}(t)$ may then be described by

$$Lf^{(1)}(t) = \kappa\omega_0^2 f^{(11)}(t) \tag{A7}$$

$$Lf^{(11)}(t) = \kappa\omega_0^2 f^{(1)}(t), \tag{A8}$$

where $L \equiv d^2/dt^2 + (\omega_0/Q)d/dt + \omega_0^2$. Equations (A7) and (A8) are adequate, as far as mode coupling is concerned, because the two normal modes given by Eq. (A6) are recovered from (A7) and (A8) when we assume normal mode solutions of the form $\exp(i\omega t)$, under the same conditions $\kappa \ll 1$ and $1/Q^2 \ll 1$. No extraneous modes are introduced, and Eqs (A7) and (A8) also have obvious interpretations in the limit $\kappa \rightarrow 0$.

APPENDIX B

THE NORMALIZED EQUATIONS

In this Appendix, we normalize the governing equations. In so doing, we identify the dimensionless parameters which need to be specified. We use a bar to denote normalized quantities, and a summary is given at the end of this Appendix.

Let $\bar{t} = \omega_0 t$, $\bar{T} = \omega_0 T$, $\bar{T}' = \omega_0 T'$, $\bar{\tau} = \omega_0 \tau$, $\bar{f} = f/f_0$, $\bar{p} = p/f_0$, and $\bar{x} = \gamma m_0 \omega_0 x/f_0$ where f_0 is the initial breakup mode amplitude in the first cavity (cf. Eq. (12)), and τ, T, T', are respectively, the beam's pulse length, the transit time between neighboring cavities within the same arm, and the transit time across a bend. We further define

$$\bar{L} \equiv d^2/d\bar{t}^2 + (1/Q)d/d\bar{t} + 1. \tag{B1}$$

Then Eq. (8) becomes

$$\bar{L}\bar{f}^{(i)}(\bar{t}) = \varepsilon_r h^{(i)}(\bar{t})\bar{x}^{(i)}(t) + \kappa\bar{f}^{(j)}(\bar{t}), \tag{B2}$$

where $i = 1, 2, 3, \ldots, 20$; $j = i + 10$ if $i \leq 10$ and $j = i - 10$ if $i \geq 11$. In Eq. (B2), $h^{(i)}$ is defined in Eq. (9) and we introduce the dimensionless constant (cf. Eq. (13))

$$\varepsilon_r = \frac{1}{\gamma}\left(\frac{I}{17kA}\right)\left(\frac{kc}{\omega_0}\right), \tag{B3}$$

which is a measure of the BBU strength in the individual beam-cavity interaction.

The beam transport Eq. (10) between adjacent cavities of the same arm is then normalized to read

$$\begin{bmatrix} \bar{x}^{(i+1)}(\bar{t} + \bar{T}) \\ \bar{p}^{(i+1)}(\bar{t} + \bar{T}) \end{bmatrix} = \bar{A} \begin{bmatrix} \bar{x}^{(i)}(\bar{t}) \\ \bar{p}^{(i)}(\bar{t}) + \bar{f}^{(i)}(\bar{t}) \end{bmatrix}, \qquad i \neq 5, 10, 15 \qquad (B4)$$

where

$$\bar{A} \equiv [\bar{a}_{ij}] = \begin{bmatrix} \cos(\Omega\bar{T}) & \Omega^{-1}\sin(\Omega\bar{T}) \\ -\Omega\sin(\Omega\bar{T}) & \cos(\Omega\bar{T}) \end{bmatrix} \qquad (B5)$$

and

$$\Omega \equiv \omega_c/\omega_0 \qquad (B6)$$

is the ratio of the effective betatron frequency (of the focusing system within the arms) to the breakup mode frequency. Similarly, the transport equation across the bend [Eq. (11)] is normalized:

$$\begin{bmatrix} \bar{x}^{(i+1)}(\bar{t} + \bar{T}') \\ \bar{p}^{(i+1)}(\bar{t} + \bar{T}') \end{bmatrix} = \bar{A}' \begin{bmatrix} \bar{x}^{(i)}(\bar{t}) \\ \bar{p}^{(i)}(\bar{t}) + \bar{f}^{(i)}(\bar{t}) \end{bmatrix}, \qquad i = 5, 10, 15 \qquad (B7)$$

where

$$\bar{A}' \equiv [\bar{a}'_{ij}] = \begin{bmatrix} \cos(\Omega'\bar{T}') & (\Omega')^{-1}\sin(\Omega'\bar{T}') \\ -\Omega'\sin(\Omega'\bar{T}') & \cos(\Omega'\bar{T}') \end{bmatrix} \qquad (B8)$$

and

$$\Omega' \equiv \omega'_c/\omega_0 \qquad (B9)$$

is the ratio of the effective betatron frequency (across the bend) to the breakup mode frequency.

We assume initial rest conditions for all $\bar{x}^{(i)}$, $\bar{p}^{(i)}$, and $\bar{f}^{(i)}$, except one, namely,

$$\bar{f}^{(1)}(0) = 1, \qquad (B10)$$

as in Eq. (12). Thus, the beam begins to pick up a non-trivial transverse displacement only when it arrives at cavity no. 2. Inserting $i = 1$ and $\bar{t} = 0$ in Eq. (B4), we obtain

$$\bar{x}^{(2)}(\bar{T}) = \bar{a}_{12}\bar{f}^{(1)}(0) = \bar{a}_{12} = \Omega^{-1}\sin(\Omega\bar{T}) \equiv x_0 \qquad (B11)$$

which is the normalized transverse displacement of the beam head when it first encounters the second cavity. All beam transverse displacement in subsequent times should be compared with the value given in Eq. (B11) to assess the BBU growth.

In summary, the normalized equations for cavity excitation are given in Eq. (B2). The beam transport is described by Eq. (B4) within each arm, and by Eq. (B7) across the bends. The *only* non-trivial initial condition is given by Eq. (B10) on the breakup mode amplitude of the first cavity. Besides the normalized time scales $\bar{t}$, $\bar{T}$, and $\bar{T}'$, we need to specify ε_r, Ω, and Ω', defined in Eqs (B3), (B6), and (B9), respectively. Normalized transverse displacement, in all cavities and for all times, should be compared with the value given in Eq. (B11) to assess the increase in the transverse displacement as a result of BBU.

REFERENCES

1. V. Bailey, L. Schlitt, M. Tiefenback, S. Putnam, A. Mondelli, D. Chernin and J. Petello, in *Proceedings of the 1987 IEEE Particle Accelerator Conf.*, Washington, DC, IEEE Cat. No. 87/CH2387-9, p. 920; S. Putnam, ibid., p. 887.
2. V. Bailey, P. Corcoran, J. Edighoffer, J. Fockler, J. Lidestri, S. Putman, and M. Tiefenback, "Status of the proof-of-concept experiment for the spiral line induction accelerator," in *Proc. Society Photo-Optical Instrumentation Engineers, SPIE* Vol. 1407, (1991).
   S. Putnam, private communication.
3. C. W. Roberson, A. Mondelli and D. Chernin, *Phys. Rev. Lett.*, **50**, 307 (1983).
4. Beam breakup is currently a very active area of research. In this paper, we follow the formulation given originally in Refs. 5, 6 for linacs. A standard reference for BBU in recirculating system is Rand's book [Ref. 7 below], while the earliest publication on BBU in recirculating accelerators is perhaps the one by P. B. Wilson and C. S. Nunan [Ref. 8]. Other related works include Refs. 9–13. Some of our recent work on linacs is given in Refs. 14–16, on strictly cyclic accelerators in Ref. 17, and discussions of the various issues in Ref. 18.
5. W. K. H. Panofsky and M. Bander, *Rev. Sci. Instrum.*, **39**, 206 (1986).
6. V. K. Neil, L. S. Hall and R. K. Cooper, *Part. Accel.*, **9**, 213 (1979).
7. R. E. Rand, *Recirculating Electron Accelerators*, Harwood Academic, Chur, Switzerland (1984), Chapter 9.
8. P. B. Wilson and C. S. Nunan, *IEEE Trans. Nucl. Sci.*, **NS-20**, 1018 (1973).
9. C. M. Lyneis, R. E. Rand, H. A. Schwettman and A. M. Vetter, *Nucl. Instrum. Meth.*, **204**, 269 (1983).
10. H. Herminghaus and H. Euteneuer, *Nucl. Instrum. Meth.*, **163**, 299 (1979).
11. J. J. Bisognano and R. L. Gluckstern, in *Proceedings of the 1987 Particle Accelerator Conf.*, Washington, DC, p. 1078.
12. G. A. Krafft and J. J. Bisognano, in *Proceedings of the 1987 Particle Accelerator Conference*, Washington, DC, p. 1356.
13. R. L. Gluckstern and F. Neri, *Part. Accel.*, **25**, 11 (1989).
14. D. G. Colombant and Y. Y. Lau, *Appl. Phys. Lett.*, **55**, 27 (1989).
15. Y. Y. Lau, *Phys. Rev. Lett.*, **63**, 1141 (1989). [Errata: **63**, 2433 (1989)]
16. D. Chernin and A. Mondelli, *Part. Accel.*, **24**, 177 (1989).
17. Y. Y. Lau and D. G. Colombant, *Appl. Phys. Lett.*, **55**, 2673 (1989).
18. D. P. Chernin, *Phys. Fluids B*. **2**, 1478, (1990).
19. B. Hui, private communication.
20. S. Penner (private communication) has stressed to us the rather different characteristics of BBU in linacs and in recirculating accelerators.
21. See. e.g., H. J. Reich, P. F. Ordung, H. L. Krauss, J. G. Skalnik, *Microwave Theory and Techniques*, Van Nostrand, New York (1953), 539.
22. Tom Genoni (private communication) recently performed numerical simulations on the BBU modes in SLIA structures. He found that when two cavities with the same characteristic frequencies are coupled, splitting of the modes does appear in the spectrum in a manner described in Eq. (5).
23. R. L. Gluckstern, F. Neri and R. K. Cooper, *Part Accel.* **23**, 53 (1988).
24. D. Chernin, *Part. Accel.*, **24**, 29 (1988).
25. B. B. Godfrey and T. P. Hughes, in *High-Brightness Accelerators*, eds. A. K. Hyder, M. F. Rose and A. H. Guenther, Plenum Press, New York (1988), 288